Modal analysis of fluid-structure interaction problems with pressure-based fluid finite elements for industrial applications

Jean-François Sigrist
DCN Propulsion, Service Technique et Scientifique, 44620 La Montagne, France

ABSTRACT
The present paper deals with numerical developments performed in the finite element code ANSYS in order to carry out coupled fluid-structure analysis with pressure-based formulation. As a result, enhancement of the modeling possibilities within ANSYS is carried out for the following fluid and fluid structure modes: i) fluid sloshing modes, ii) fluid and fluid-structure modes with pressure-displacement formulation in axi-symmetric geometry with non axi-symmetric loading, iii) fluid-structure modes with symmetric formulations for elasto-acoustic and hydro-elastic problems, using the so-called symmetric (u, p, φ) and (u, η, φ) formulations. The paper also aims at providing finite element code users with test cases to refer to, for application of the new FSI formulations. The paper also serves as an introduction to the numerical calculation of eigenvalue problems with FSI. Theoretical bases of the formulations are first exposed; test-cases and industrial applications are then proposed. It is shown in particular that computing times are significantly decreased by using a symmetric formulation instead of a non-symmetric one, allowing modal analysis of complex structures with fluid coupling for industrial purposes.

Key-words: Fluid-Structure Interaction; Fluid Finite Elements; Modal Analysis; Symmetric Formulations; Finite Element Code Validation

INTRODUCTION

The present paper deals with the numerical simulation of "fluid-structure interaction" problems (Axisa, 2006a ; Morand-Ohayon, 1995): it is concerned with the elastic behavior of a structure in contact with an inviscid fluid that vibrates about a stagnant state. Problems involving a deformable structure coupled with a fluid with non stationary flow are referred to as "flow induced vibration" coupled problems (Axisa, 2006b ; Païdoussis, 1998 ; Païdoussis, 2003). In the latter case, numerical simulation of the coupled problem requires the calculation of the structure displacement field and the fluid pressure and velocity fields in the space-time domain. Moreover, some problems need solving non linear equations for the fluid and/or structure domains (Schäfer-Teschauer, 2001). In the former case, the structure and fluid are supposed to have linear behavior and are then described within the framework of elastic vibrations. As a consequence, numerical calculation of the coupled problem can then be performed in the frequency domain. Many numerical methods, mostly finite element and boundary element methods have been proposed to take these FSI effects into account in various engineering domains (Mackerle, 1999). Such methods have been firmly validated from the theoretical, numerical and even experimental points of view, and their application to industrial problems for design purposes is still an actual concern (Sigrist, 2006).

The ANSYS code (Khonke, 1986), of wide use in industry and academia, did not allow up to now to perform dynamic analysis of coupled fluid-structure systems using efficient calculation procedures, because the formulation of the coupled problem in ANSYS involves non-symmetric matrices (Woyak, 1995). Formulations involving symmetric matrices are known to be less costly from the computational point of view. They also allow the use of modal decomposition techniques for the dynamic analysis of coupled systems, since eigenmodes calculated with symmetric operators fulfill orthogonality conditions required by the modal approach (Bathe, 1982).

The present paper exposes numerical developments undertaken in order to enhance the existing fluid elements in the ANSYS code in order to tackle fluid-structure interaction modeling for industrial applications. These numerical developments bring out new functionalities in future releases of the code, with the view to computing:

- Fluid sloshing modes with pressure-based formulation,
- Fluid and fluid-structure modes with pressure-displacement formulation in axi-symmetric geometry with non axi-symmetric loading,
- Fluid-structure modes with symmetric formulations for elasto-acoustic and hydro-elastic problems, using the so-called symmetric (u, p, φ) and (u, η, φ) formulations (Morand-Ohayon, 1995).

The paper gives validation test cases which have been studied before these new formulations be available in future release of the code. The paper also aim at providing users of the ANSYS code - as well as other finite element code - with test cases to refer to, for application of the new FSI formulations. The paper also serves as an introduction to the numerical calculation of eigenvalue problems with FSI for industrial application. Theoretical bases of the above mentioned formulations are exposed in the second subsection, elementary validation test-cases are proposed in the third subsection and an industrial application is presented in the last subsection.

Practical applications of the presented developments within the ANSYS code cover a wide range of industrial problems for instance in automotive, aeronautic and shipbuilding industries. In the particular field of nuclear power engineering, the present developments will make it possible to use the ANSYS code for the calculation of the dynamic response of structures to seismic solicitation with FSI modeling, using modal methods, such approaches being of paramount importance in seismic design (Sigrist-Broc, 2006).

1. FLUID-STRUCTURE INTERACTION MODELING WITH FLUID PRESSURE-BASED AND DISPLACEMENT-BASED FORMULATIONS

1.1. LINEAR FLUID MODELING WITH PRESSURE-BASED OR DISPLACEMENT BASED EQUATIONS

In the general case, the fluid flow is described by the Navier-Stokes equations which read:

$$\frac{\partial \rho}{\partial t} + \frac{\partial(\rho v_j)}{\partial x_i} = 0 \qquad (1)$$

$$\frac{\partial(\rho v_i)}{\partial t}+\frac{\partial(\rho v_i v_j)}{\partial x_j}=-\frac{\partial p}{\partial x_i}+\mu\frac{\partial^2 v_i}{\partial x_j^{\,2}} \tag{2}$$

where $\mathbf{v}$ = (vi) and p are the fluid velocity and pressure field. ρ and μ stand for the fluid density and viscosity respectively. The mass and momentum conservation equations are to be solved together with the fluid state equation which reads:

$$p = p(\rho) \tag{3}$$

In the framework of fluid-structure interaction problems, the fluid is supposed to be inviscid and initially at rest in a steady state characterized by a pressure field p_0 ($\mathbf{x}$) a velocity field $\mathbf{v}_0 = \mathbf{0}$ and constant density ρ_0. In a linear description of the fluid behavior, fluctuations of pressure, velocity and density about the steady state is accounted for using the following decomposition:

$$p(\mathbf{x},t) = p_o(\mathbf{x}) + p'(\mathbf{x},t) \qquad \rho(\mathbf{x},t) = \rho_o + \rho'(\mathbf{x},t) \tag{4}$$

where fluctuating part of the pressure and density are denoted p' and ρ' respectively.
Linearization of the fluid state law equation reads:

$$p' = c_o^2 \rho' \tag{5}$$

where $c_o = \sqrt{\left.\frac{\partial p}{\partial \rho}\right|_{(p_o,\rho_o)}}$ is the velocity of the pressure waves within the fluid media.

The pressure and density fields as written in Eq. (4) are substituted in Eqs. (1) and (2), in which the viscosity term has been discarded. Retaining the first order terms and taking into account Eq. (5) then yields:

$$\frac{1}{c_o^2}\frac{\partial p'}{\partial t}+\rho_o\frac{\partial v_j}{\partial x_j}=0 \tag{6}$$

$$\frac{\partial p'}{\partial x_i}=-\rho_o\frac{\partial v_i}{\partial t} \tag{7}$$

Taking the divergence of Eq. (7) and combining with a time derivation of Eq. (6) yields:

$$\frac{1}{c_o^2}\frac{\partial^2 p'}{\partial t^2}-\frac{\partial^2 p'}{\partial x_j^2}=0 \tag{8}$$

which describes the propagation of acoustic waves within the fluid.
In the linear approach, the fluid can also be described with a displacement field ξ, the velocity field being $\mathbf{v} = \frac{\partial \xi}{\partial t}$. Pressure can be calculated from displacement:

time integration of Eq. (6) indeed yields:

$$p' = -\rho_0 c_0^2 \frac{\partial \xi_j}{\partial x_j} \tag{9}$$

Boundary condition describing the coupling with a moving wall is expressed with the non slip condition:

$$\boldsymbol{\xi} \cdot \mathbf{n} = \mathbf{d} \cdot \mathbf{n} \tag{10}$$

where **d** is the wall displacement. Taking Eq. (7) into account, the boundary condition can also be formulated in terms of pressure:

$$\nabla p' \cdot \mathbf{n} = -\rho_o \frac{\partial^2 \mathbf{d}}{\partial t^2} \cdot \mathbf{n} \tag{11}$$

where **n** is the unit normal to the moving wall.

Boundary condition describing a fluid free surface is simply written:

$$p' = 0 \tag{12}$$

in the case of non weighting fluid, i.e. when gravity effects are discarded.

Gravity (or "sloshing") effects are accounted for with the condition:

$$p' = \rho_0 g \eta \tag{13}$$

where η is the free surface elevation, that is the fluid displacement in the direction normal to the fluid free surface. Using a second order time derivation of Eq. (13) and taking into account Eq. (7) finally yields an equivalent boundary condition for fluid sloshing in terms of fluid pressure:

$$\nabla p \cdot \mathbf{n} = -\frac{1}{g} \frac{\partial^2 p}{\partial t^2} \tag{14}$$

where **n** is the unit ascending normal to the free surface, so that gravity field is $\mathbf{g} = -g\mathbf{n}$.

The pressure and displacement formulation of the elastic fluid behavior as described by the previous equations corresponds to the modeling approach in the ANSYS code, except for sloshing modeling which is not implemented in the code. Coupling of the fluid with the structure is then described as follows.

1.2. COUPLED FLUID-STRUCTURE PROBLEM WITH PRESSURE-BASED FLUID FORMULATION

The general equations of the coupled fluid-structure problem using a pressure-based formulation for the fluid are written in the frequency domain. Figure 1 gives a generic representation of the coupled problem. Let Ω_s be the structure domain with boundary $\partial\Omega_s = \partial\Omega_{s\sigma} \cup \partial\Omega_{so} \cup \Gamma$ where $\partial\Omega_{s\sigma}$ is the boundary part with imposed forces, $\partial\Omega_{so}$ is the boundary part with imposed displacement and Γ is the fluid-structure interface. $\mathbf{n}_s$ is the outward normal on $\partial\Omega_s$ $\mathbf{n}$ is the inward normal on Γ. $\mathbf{u}$ is the structure displacement, $\sigma(\mathbf{u})$ is the stress tensor. ρ_s stands for structure density. The structure problem equations in displacement formulation read:

$$-\omega^2 \rho_S u_i - \frac{\partial \sigma_{ij}(\mathbf{u})}{\partial x_j} = 0 \text{ in } \Omega_S \tag{15}$$

$$u_i = 0 \text{ on } \partial\Omega_{So} \tag{16}$$

$$\sigma_{ij}(\mathbf{u}) n_j^S = 0 \text{ on } \partial\Omega_{S\sigma} \tag{17}$$

$$\sigma_{ij}(\mathbf{u}) n_j^S = p n_i \text{ on } \Gamma \tag{18}$$

Let Ω_F be the fluid domain with $\partial\Omega_F = \partial\Omega_{Fo} \cup \partial\Omega_{so} \cup \Gamma$, where $\partial\Omega_{F\pi}$ is the boundary part with imposed normal gradient pressure (rigid wall or symmetry plane), $\partial\Omega_{Fo}$ the boundary part with imposed pressure (pressure release surface or anti-symmetry plane) and Γ is the structure-fluid interface. $\mathbf{n}_F$ is the outward normal on $\partial\Omega_F$, n is the outward normal on Γ. In order to alleviate the notation, the fluid fluctuating pressure field is now denoted p instead of p\`. In the same manner, fluid density and velocity waves are denoted ρ_F and c respectively (instead of ρ_0). Using the linear equations developed in the previous subsection, the pressure-base fluid equations in the frequency domain read:

$$-\frac{\omega^2}{c^2} p - \frac{\partial^2 p}{\partial x_i^2} = 0 \text{ in } \Omega_F \tag{19}$$

$$\frac{\partial p}{\partial x_j} n_j^F = 0 \text{ on } \partial\Omega_{F\pi} \tag{20}$$

$$p = 0 \text{ on } \partial\Omega_{Fo} \tag{21}$$

$$\frac{\partial p}{\partial x_i} n_i = \rho_F \omega^2 u_i n_i \text{ on } \Gamma \tag{22}$$

Coupling conditions between the structure and fluid problems are given by Eqs. (18) and (22). Equation (18) expresses the continuity of the normal component of the stress tensor at the fluid-structure interface. On Γ, fluid acts on structure *via* an imposed pressure that creates a structure loading in the normal direction at the structure boundary . Equation (22) expresses the continuity of the displacement normal component. On Γ, structure acts on fluid via an imposed displacement in the normal direction at the fluid boundary.

Numerical resolution of the coupled problem is obtained with a discretization procedure of the variationnal formulation of the fluid-structure interaction problem. On the one hand, the structure problem is written as:

$$\int_{\Omega_S} \sigma_{ij}(\mathbf{u})\varepsilon_{ij}(\delta\mathbf{u}) - \omega^2 \int_{\Omega_S} \rho_S u_i \delta u_i - \int_{\Gamma} p n_i \delta u_i = 0 \tag{23}$$

for any virtual displacement field $\delta\mathbf{u}$ which complies with boundary condition (16). On the other hand, the fluid problem is written:

$$\int_{\Omega_F} \frac{\partial p}{\partial x_i}\frac{\partial \delta p}{\partial x_i} - \omega^2 \int_{\Omega_F} \frac{p\delta p}{c^2} - \rho_F \omega^2 \int_{\Gamma} u_i n_i \delta p = 0 \tag{24}$$

for any virtual pressure field δp satisfying boundary condition (21).

Spatial discretization of Eqs. (23) and (24) is performed with finite elements (Bathe, 1982; Morand-Ohayon, 1995). Mass and stiffness matrices of the fluid and structure problem are defined as:

$$\int_{\Omega_S} \rho_S u_i \delta u_i \rightarrow \delta\mathbf{U}^T \mathbf{M}_S \mathbf{U} \tag{25}$$

$$\int_{\Omega_S} \sigma_{ij}(\mathbf{u})\varepsilon_{ij}(\delta\mathbf{u}) \rightarrow \delta\mathbf{U}^T \mathbf{K}_S \mathbf{U} \tag{26}$$

$$\int_{\Omega_F} \frac{\partial p}{\partial x_i}\frac{\partial \delta p}{\partial x_i} \rightarrow \delta\mathbf{P}^T \mathbf{K}_F \mathbf{P} \tag{27}$$

$$\int_{\Omega_F} \frac{p\delta p}{c^2} \rightarrow \delta\mathbf{P}^T \mathbf{M}_F \mathbf{P} \tag{28}$$

Fluid-structure interaction matrices are used to model coupled terms and are defined as:

$$\int_{\Gamma} p n_i \delta u_i d\Gamma \rightarrow \delta\mathbf{U}^T \mathbf{R}\mathbf{P} \qquad \int_{\Gamma} u_i n_i \delta p d\Gamma \rightarrow \delta\mathbf{P}^T \mathbf{R}^T \mathbf{U} \tag{29}$$

Finally, the coupled problem takes the following form:

$$\begin{bmatrix} \mathbf{K}_S & -\mathbf{R} \\ 0 & \mathbf{K}_F \end{bmatrix} \begin{Bmatrix} \mathbf{U}(\omega) \\ \mathbf{P}(\omega) \end{Bmatrix} = \omega^2 \begin{bmatrix} \mathbf{M}_S & \mathbf{0} \\ \rho_F \mathbf{R}^T & \mathbf{M}_F \end{bmatrix} \begin{Bmatrix} \mathbf{U}(\omega) \\ \mathbf{P}(\omega) \end{Bmatrix} \tag{30}$$

The displacement-pressure formulation leads to a non-symmetric eigenvalue problem which can be solved with the non-symmetric Lanczos algorithm (Rajakumar-Rogers, 1991), which requires important computational time. As a consequence, the modal analysis of complex structures with fluid-structure interaction modeling is practically out of reach for industrial applications.

1.3. DISPLACEMENT-BASED FLUID FORMULATION

Using a displacement-based formulation for both fluid and structure problems yields a symmetric coupled formulation. Using notations of the preceding subsection, equations of the structure problem remain unchanged, while equations for the fluid problem in the frequency domain read (see subsection 1.1):

$$\frac{\omega^2}{c^2}\xi_i + \frac{\partial}{\partial x_i}\left(\frac{\partial \xi_j}{\partial x_j}\right) = 0 \text{ in } \Omega_F \tag{31}$$

$$\xi_j n_j^F = 0 \text{ on } \partial\Omega_{F\pi} \tag{32}$$

$$\frac{\partial \xi_j}{\partial x_j} = 0 \text{ on } \partial\Omega_{Fo} \tag{33}$$

Coupling conditions (18) and (22) are now replaced by the following equations:

$$u_i n_i = \xi_i n_i \text{ on } \Gamma \tag{34}$$

$$\sigma_{ij}(\mathbf{u}) n_j^S = -\rho_F c^2 \frac{\partial \xi_j}{\partial x_j} n_i \text{ on } \Gamma \tag{35}$$

which express the continuity of the normal component of the stress tensor and displacement fields at the fluid-structure interface. Variationnal formulation of the problem reads:

$$\int_{\Omega_F} \rho_F c^2 \frac{\partial \xi_i}{\partial x_i}\frac{\partial \delta\xi_i}{\partial x_i} + \int_{\Omega_S} \sigma_{ij}(\mathbf{u})\varepsilon_{ij}(\delta\mathbf{u}) - \omega^2 \int_{\Omega_F} \rho_F \xi_i \delta\xi_i - \omega^2 \int_{\Omega_S} \rho_S u_i \delta u_i = 0 \tag{36}$$

for any structure virtual displacement field $\delta\mathbf{u}$ and any fluid virtual displacement field $\delta\xi$ that comply with respectively with boundary conditions (16) and (32), and coupling condition (34). Finite element discretization of Eq. (36) yields the following eigenvalue problem:

$$\left(\begin{bmatrix} \mathbf{K}_S & \mathbf{0} \\ \mathbf{0} & \hat{\mathbf{K}}_F \end{bmatrix} - \omega^2 \begin{bmatrix} \mathbf{M}_S & \mathbf{0} \\ \mathbf{0} & \hat{\mathbf{M}}_F \end{bmatrix}\right) \begin{Bmatrix} \mathbf{U}(\omega) \\ \mathbf{X}(\omega) \end{Bmatrix} = \begin{Bmatrix} \mathbf{0} \\ \mathbf{0} \end{Bmatrix} \tag{37}$$

where matrices $\hat{\mathbf{K}}_F$ and $\hat{\mathbf{M}}_F$ and discretize the bilinear forms $\int_{\Omega_F} \rho_F c^2 \frac{\partial \xi_i}{\partial x_i} \frac{\partial \delta\xi_i}{\partial x_i}$ and $\int_{\Omega_F} \rho_F \xi_i \delta\xi_i$ respectively. Equation (37) involves symmetric matrices but from the practical point of view, the use of the (**u**, ξ) coupled formulation suffers from major drawbacks since it produces non physical spurious modes which correspond to rotational motions within the fluid. Moreover, the kinetic and potential energy associated with these spurious modes can be different from zero: this can significantly affect the numerical results in dynamic analysis with modal decomposition techniques. Such problems could be overcome either by discretizing the condition **curl**(ξ) = 0 for the fluid displacement field (Hamdi et al., 1978), or by using alternate coupling conditions (Bermudez et al., 1998, 1995 ; Bermudez et al., 1998). However, none of these approaches can easily be applied to the ANSYS code.

1.4. FLUID AND FLUID-STRUCTURE ANALYSIS WITH THE ANSYS CODE

Table 1 summarizes the various analysis possibilities offered by the ANSYS code in terms of fluid or fluid-structure problems with the pressure-displacement and displacement-displacement formulations. The (**u**, ξ) formulation allows all kind of analysis, including dynamic analysis with modal decomposition techniques. However, as mentioned above, such formulation is of difficult use from the engineering standpoint. Besides, physical interpretation of fluid modes in terms of displacement is not straightforward in comparison with the pressure formulation.

Numerical developments are then undertaken in ANSYS in order to use pressure-based formulation for fluid and fluid-structure analysis with calculation of:

- Fluid sloshing modes with pressure-based formulation,
- Fluid and fluid-structure modes with pressure-displacement formulation in axi-symmetric geometry with non axi-symmetric loading,
- Fluid-structure modes with symmetric formulations for elasto-acoustic and hydro-elastic problems.

2. NUMERICAL DEVELOPMENTS WITHIN THE ANSYS CODE

2.1. SLOSHING WITH FLUID PRESSURE-BASED ELEMENTS

Using the notations of Fig. 1, formulation of a fluid sloshing problem in terms of pressure is given by the following equations (Biswal et al., 2002):

$$\frac{\partial^2 p}{\partial x_i^2} = 0 \text{ in } \Omega_F \tag{38}$$

$$\frac{\partial p}{\partial x_j} n_j^F = \frac{\omega^2}{g} p \text{ on } \partial\Omega_{Fo} \tag{39}$$

$$\frac{\partial p}{\partial x_j} n_j^F = 0 \text{ on } \partial\Omega_{F\pi} \tag{40}$$

As sloshing modes are in the low frequency range, fluid compressibility is discarded in the analysis; therefore, Eq. (38) exhibits the incompressible behavior of the fluid. The free surface condition is described by Eq. (39), in which the normal vector $\mathbf{n}_F$ is oriented in the vertical ascendant direction.

Variationnal formulation of the problem is then:

$$\omega^2 \int_{\partial\Omega_{Fo}} \frac{p\delta p}{g} + \int_{\Omega_F} \frac{\partial p}{\partial x_i}\frac{\partial \delta p}{\partial x_i} = 0 \tag{41}$$

for any fluid virtual pressure field δp. Discretization of the free surface terms yields a fluid mass matrix $\mathbf{M}'_F$ defined as follows:

$$\int_{\partial\Omega_{Fo}} \frac{p\delta p}{g} \rightarrow \delta\mathbf{P}^T \mathbf{M}'_F \mathbf{P} \tag{42}$$

Calculation of the sloshing modes is performed by solving the eigenvalue problem:

$$(-\omega^2 \mathbf{M}'_F + \mathbf{K}_F)\mathbf{P}(\omega) = \mathbf{0} \tag{43}$$

In the ANSYS code, pressure based fluid elements fluid29 and fluid30 for 2D-axi and 3D problems are then enhanced to take into account fluid sloshing modes. Validation of sloshing mode calculation is presented in the next subsection in 3D and 2D-axi symmetric cases.

2.2. HARMONIC AXI-SYMMETRIC FLUID PRESSURE-BASED ELEMENT

In some industrial application, many structures can be modeled using an axi-symmetric assumption, while dynamic loading on structures can be non axi-symmetric: this is the case in particular for nuclear pressure vessels subjected to seismic solicitation (Sigrist-Broc, 2006). Harmonic axi-symmetric representation of the problem unknown with a Fourier serie is then of convenient use. In the ANSYS code, such an approach is possible only with structure shell or solid elements (Khonke, 1986). As for the fluid pressure elements, implementation of an harmonic axi-symmetric formulation is obtained as follows. The pressure unknown is expanded as a Fourier serie according to:

$$p(r,\theta,z) = p^0(r,z) + \sum_{s\geq 1} p^s(r,z)\cos(s\theta) + \sum_{a\geq 1} p^a(r,z)\sin(a\,\theta) \tag{44}$$

As stated by Eq. (44), dependency of the pressure with respect to θ is taken into account with the trigonometric functions $\cos(s\theta)$ and $\sin(a\theta)$, while dependency with respect to r and z is accounted for with the pure axi-symmetric component p^o and symmetric and anti-symmetric components of the pressure field p^s and p^a. Discretization of the problem is then performed in the (r,z) plane, where the fluid domain is denoted as $\hat{\Omega}_F$ using four-nodes, one-degree-of-freedom fluid elements, as depicted by Fig. 2. The associated shape functions are linear with respect to the r and z directions. On the reference element local coordinates are denoted by ξ and η. Shape function for node ie [1,4] is:

$$N_i^F(\xi,\eta) = \frac{(1+\xi_i\xi)(1+\eta_i\eta)}{4} \quad (45)$$

Calculation of the fluid mass matrices is:

$$\mathbf{M}_F = \int_{\hat{\Omega}_F} \frac{\{N_F\}\langle N_F\rangle}{c^2} r dr dz \quad (46)$$

for the compressibility effects, and:

$$\mathbf{M'}_F = \int_{\partial\hat{\Omega}_{Fo}} \frac{\{N_F\}\langle N_F\rangle}{g} r dr dz \quad (47)$$

for the sloshing effects. Calculation of the fluid stiffness matrix corresponding to the symmetric component of order s ≥ 0 is given by:

$$\mathbf{K}_F = \mathbf{K}_F^o + s^2 \mathbf{K}_F^s \quad (48)$$

where $\mathbf{K}_F^o$ and $\mathbf{K}_F^s$ are defined by:

$$\mathbf{K}_F^o = \int_{\hat{\Omega}_F} \left(\frac{\partial\{N_F\}}{\partial r}\frac{\partial\langle N_F\rangle}{\partial r} + \frac{\partial\{N_F\}}{\partial z}\frac{\partial\langle N_F\rangle}{\partial z}\right) r dr dz \quad (49)$$

$$\mathbf{K}_F^s = \int_{\hat{\Omega}_F} \{N_F\}\langle N_F\rangle \frac{dr dz}{r} \quad (50)$$

Similar expression can be derived for any anti-symmetric component a ≥ 1.

The matrices are assembled with the elementary mass and stiffness matrices which can be analytically calculated according to the following expressions, using notations of Fig. 2 (Sigrist et al., 2004):

$$\mathbf{m}_F(i,j) = \frac{ab}{4c^2}\left[r_0 + \frac{r_0\xi_i\xi_j}{3} + \frac{a(\xi_i+\xi_j)}{3}\right] \times \left[1 + \frac{\eta_i\eta_j}{3}\right] \quad (51)$$

$$\mathbf{m'}_F(i,j) = \frac{a}{g}\left[r_0 + \frac{r_0\xi_i\xi_j}{3} + \frac{a(\xi_i+\xi_j)}{3}\right] \times \left[(1+\eta_i)(1+\eta_j)\right] \quad (52)$$

$$\mathbf{k}_F^o(i,j) = abr_0\left[\frac{\xi_i\xi_j}{4a^2}(1+\frac{\eta_i\eta_j}{3}) + \frac{\eta_i\eta_j}{4a^2}(1+\frac{\xi_i\xi_j}{3})\right] + \frac{a^2\eta_i\eta_j}{12b}(\xi_i+\xi_j) \quad (53)$$

$$\mathbf{k}_F^s(i,j) = \frac{b}{8}\left[1+\frac{\eta_i\eta_j}{3}\right]\times\left[2(\xi_i+\xi_j)-\frac{2r_0\xi_i\xi_j}{a}+\left(1-\frac{r_0(\xi_i+\xi_j)}{a}+\frac{r_0^{\,2}\xi_i\xi_j}{a^2}\right)\times ln\left(\frac{r_0+a}{r_0-a}\right)\right] \quad (54)$$

In the ANSYS code, 2D-axisymmetric modeling of fluid problems is produced with the pressure-base fluid element fluid29. The harmonic axi-symmetric case is taken into account with a specific key-option of the element, that activates the calculation of mass and stiffness matrices according to Eqs. (47) to (50). Validation of this functionality is presented in the next subsection.

2.3. SYMMETRIC COUPLED FORMULATIONS FOR HYDRO-ELASTIC AND ELASTO-ACOUSTIC PROBLEMS

As recalled in subsection 1.2, the displacement-pressure coupled formulation leads to non-symmetric eigenvalue mass and stiffness matrices, requiring higher computational time in eigenvalue calculation. Besides, modal decomposition techniques can not be applied in a straightforward manner with eigenmodes calculated from non-symmetric eigenvalue problem. Symmetric formulations for fluid-structure interaction problems can be derived, for instance using three fields formulations (Kanarachos-Antoniadis, 1988) or modal reduction techniques (Ohayon, 2001). As for the ANSYS code, three field formulations have been implemented and validated for industrial applications.

a) Elasto-acoustic problem

For elasto-acoustic problems (i.e. problems involving an elastic structure coupled with an acoustic fluid), the three-field ($\mathbf{u}$,p,φ) formulation (Axisa-Gibert, 1982 ; Ohayon-Valid, 1983) yields a symmetric coupled problem, by using the fluid displacement potential defined as:

$$\boldsymbol{\xi} = \nabla\varphi \quad (55)$$

Taking Eq. (7) into account yields:

$$p = -\rho_F\frac{\partial^2\varphi}{\partial t^2} \quad (56)$$

Formulation of the coupled problem is then written as follows. The equations of the structure problem in the frequency domain are unchanged, except for coupling condition (18) which becomes:

$$\sigma_{ij}(u)n_j^S = \rho_F\omega^2\varphi n_i \ \text{ on } \Gamma \quad (57)$$

As for the fluid problem, the acoustic wave propagation is described by the mixed pressure/displacement potential equations:

$$-\frac{\omega^2}{c^2}\varphi+\frac{p}{\rho_F c^2}=0 \qquad \rho_F\frac{\partial^2\varphi}{\partial x_i^2}+\frac{p}{c^2}=0 \qquad \text{in } \Omega_F \quad (58)$$

with free surface condition and rigid wall condition expressed in terms of displacement potential as:

$$\varphi = 0 \text{ on } \partial\Omega_{Fo} \tag{59}$$

$$\frac{\partial\varphi}{\partial x_j} n_j^F = 0 \text{ on } \partial\Omega_{F\pi} \tag{60}$$

The coupling condition with the elastic structure reads:

$$\frac{\partial\varphi}{\partial x_j} n_j^F = u_i n_i \tag{61}$$

Variationnal formulation of the problem reads:

$$\omega^2 \int_{\Omega_S} \rho_S u_i \delta u_i + \int_{\Omega_S} \sigma_{ij}(\mathbf{u}) \varepsilon_{ij}(\delta\mathbf{u}) = \rho_F \omega^2 \int_{\Gamma} \varphi n_i \delta u_i \tag{62}$$

$$\rho_F \int_{\Omega_F} \frac{\partial\varphi}{\partial x_i}\frac{\partial\delta\varphi}{\partial x_i} + \int_{\Omega_F} \frac{p\delta\varphi}{c^2} + \rho_F \int_{\Omega_F} u_i n_i \delta\varphi = 0 \tag{63}$$

$$\frac{1}{\rho_F} \int_{\Omega_F} \frac{p\delta p}{c^2} - \omega^2 \int_{\Omega_F} \frac{\varphi\delta p}{c^2} = 0 \tag{64}$$

for any virtual fields $\delta\mathbf{u}$, $\delta\varphi$ and δp complying with boundary conditions. Finite element discretization of Eqs. (62) to (64) with finite elements using the same shape functions for pressure and displacement potential yields the matricial system:

$$\begin{bmatrix} \mathbf{K}_S & \mathbf{0} & \mathbf{0} \\ \mathbf{0} & 1/\rho_F \mathbf{M}_F & \mathbf{0} \\ \mathbf{0} & \mathbf{0} & \mathbf{0} \end{bmatrix} \begin{Bmatrix} \mathbf{U}(\omega) \\ \mathbf{P}(\omega) \\ \mathbf{\Phi}(\omega) \end{Bmatrix} = \omega^2 \begin{bmatrix} \mathbf{M}_S & \mathbf{0} & \rho_F \mathbf{R} \\ \mathbf{0} & \mathbf{0} & \mathbf{M}_F \\ \rho_F \mathbf{R}^T & \mathbf{M}_F & -\rho_F \mathbf{K}_F \end{bmatrix} \begin{Bmatrix} \mathbf{U}(\omega) \\ \mathbf{P}(\omega) \\ \mathbf{\Phi}(\omega) \end{Bmatrix} \tag{65}$$

The mass and stiffness matrices in Eq. (65) are symmetric and involves the structure, fluid and coupling operators used in the non-symmetric formulation. Elimination of the unknown Φ in Eq. (65) can be obtained with a condensation procedure. Third line of Eq. (65) yields:

$$\mathbf{\Phi}(\omega) = \mathbf{K}_F^{-1} \mathbf{R}^T \mathbf{U}(\omega) + 1/\rho_F \mathbf{K}_F^{-1} \mathbf{M}_F \mathbf{P}(\omega) \tag{66}$$

Whence the condensed symmetric forms in term of pressure and displacement:

$$\begin{bmatrix} \mathbf{K}_S & \mathbf{0} \\ \mathbf{0} & 1/\rho_F \mathbf{M}_F \end{bmatrix} \begin{Bmatrix} \mathbf{U}(\omega) \\ \mathbf{P}(\omega) \end{Bmatrix} = \omega^2 \begin{bmatrix} \mathbf{M}_S + \rho_F \mathbf{R}\mathbf{K}_F^{-1}\mathbf{R}^T & \mathbf{R}\mathbf{K}_F^{-1}\mathbf{M}_F \\ \mathbf{M}_F \mathbf{K}_F^{-1} \mathbf{R}^T & 1/\rho_F \mathbf{M}_F \mathbf{K}_F^{-1} \mathbf{M}_F \end{bmatrix} \begin{Bmatrix} \mathbf{U}(\omega) \\ \mathbf{P}(\omega) \end{Bmatrix} \tag{67}$$

Formulation (65) involves symmetric sparse matrices, whereas formulation (67) involves symmetric full matrices. In ANSYS, Eq. (65) is solved as such with the block Lanczos algorithm, while Eq. (67) is solved after a condensation step using the Guyan procedure.

b) Hydroelastic-sloshing problem

For hydroelastic-sloshing problems (i.e. problems involving an elastic structure coupled with a incompressible fluid with sloshing effects), the three-field ($\mathbf{u},\eta,\varphi$) formulation (Morand-Ohayon, 1995) yields a symmetric coupled problem, using the fluid free surface elevation η and the fluid displacement potential.

Equations of the structure problem are given by Eqs.(15) to (17) using pressure loading on structure through the relation $p = \rho_F g\eta$. Equations of the fluid problem are:

$$\frac{\partial^2\varphi}{\partial x_j^2} = 0 \text{ in } \Omega_F \tag{68}$$

$$\omega^2\varphi + g\eta = 0 \qquad \frac{\partial\varphi}{\partial x_j} n_j^F = \eta \text{ on } \partial\Omega_{Fo} \tag{69}$$

Boundary condition for rigid wall and coupling condition with the structure are given by Eqs. (60) and (61), respectively. Variationnal formulation of the problem is given by Eq. (62) for the structure and:

$$-\omega^2 \int_{\partial\Omega_{Fo}} \varphi\delta\eta + \int_{\partial\Omega_{Fo}} g\eta\delta\eta = 0 \tag{70}$$

$$\rho_F \int_{\Omega_F} \frac{\partial\varphi}{\partial x_i}\frac{\partial\delta\varphi}{\partial x_i} + \rho_F \int_{\Gamma} u_i n_i \delta\varphi + \rho_F \int_{\partial\Omega_{Fo}} \eta\delta\varphi = 0 \tag{71}$$

for the fluid problem. Discretization of the free-surface integrals terms yields the following operators:

$$\int_{\partial\Omega_{Fo}} g\eta\delta\eta \rightarrow \delta\mathbf{H}^T\tilde{\mathbf{K}}_F\mathbf{H} \tag{72}$$

$$\int_{\partial\Omega_{Fo}} \eta\delta\varphi \rightarrow \delta\mathbf{\Phi}^T\tilde{\mathbf{M}}_F\mathbf{H} \tag{73}$$

The eigenvalue problem finally reads:

$$\begin{bmatrix} \mathbf{K}_S & \mathbf{0} & \mathbf{0} \\ \mathbf{0} & \tilde{\mathbf{K}}_F & \mathbf{0} \\ \mathbf{0} & \mathbf{0} & \mathbf{0} \end{bmatrix} \begin{Bmatrix} \mathbf{U}(\omega) \\ \mathbf{H}(\omega) \\ \mathbf{\Phi}(\omega) \end{Bmatrix} = \omega^2 \begin{bmatrix} \mathbf{M}_S & \mathbf{0} & \rho_F\mathbf{R} \\ \mathbf{0} & \mathbf{0} & \tilde{\mathbf{M}}_F \\ \rho_F\mathbf{R}^T & \tilde{\mathbf{M}}^T{}_F & -\rho_F\mathbf{K}_F \end{bmatrix} \begin{Bmatrix} \mathbf{U}(\omega) \\ \mathbf{H}(\omega) \\ \mathbf{\Phi}(\omega) \end{Bmatrix} \tag{74}$$

which has the same form as Eq. (65) for the acoustic problem. Condensation of Φ in Eq. (74) yields a symmetric formulation in terms of structure displacement and fluid free surface elevation, with matrix system similar to (67).

3. VALIDATION TEST CASES

3.1. HYDROELASTIC-SLOSHING CASE

Validation of the developments in the ANSYS code for hydroelastic-sloshing calculation is performed on the elementary test case sketched by Fig. 3. 3D and 2D axi-symmetric calculation will be compared on the studied case. The geometrical and physical parameters of the problem are as follows: R = 0.1m, $R = \alpha R$ = 0.2 m, $L = H$ = 0.75m, e = 0.01m, ρ_s = 7800 kg/m^3 , E = 2.1 10^6 Pa^1, υ = 0.3, ρ_F = 1000 kg/m^3, g = 9.81 m/s^2. Fluid mesh is produced with N_r = 10, N_θ = 15 and N_z = 20 elements in the r, θ and z directions respectively.

a) Fluid problem

For the studied case, eigenfrequencies of the fluid sloshing modes can be analytically computed according to:

$$f_{m,n} = \frac{1}{2\pi}\sqrt{g q_{n,m} / R \times \tanh(q_{n,m} H / R)} \tag{75}$$

where $q_{n,m}$ is the th m^{th} root of $D_{n,\alpha}(x) = J'_n(x)\, Y'_n(\alpha x) - J'_n(\alpha x)\, Y'_n(x)$ (see appendix A). Index n stands for the dependence of pressure in the θ direction and index m stands for the eigenmode order.

2D-axi symmetric, 3D and analytical calculations of eigenfrequencies are compared in Tab. 2. Figure 4 sketches the corresponding eigenmodes shapes in terms of pressure distribution for the 2D and 3D model. 2D and 3D calculations give equivalent results, with no noticeable discrepancy to the analytical solution. The third and fourth frequencies computed with the 2D-axi or 3D models are nonetheless overestimated with the standard mesh; convergence is however obtained with the mesh refinement, as represented in Fig. 5 for 2D-axi calculations. Same trends are also observed for other sloshing modes (corresponding to s > 1 and a > 1).

b) Coupled fluid-structure problem

Calculations are then performed for the coupled fluid-structure problem using 2D axi-symmetric and 3D models together with symmetric and non symmetric formulations. As the decoupled frequencies of the structure (elastic modes) and the fluid (sloshing modes) are close to each other, strong coupling effects are expected. Table 3 gives the computed frequencies for hydroelastic-sloshing coupled eigenmodes, and compares the various calculations for symmetric modes of order one (i.e. corresponding to s = 1 in the axi-symmetric case). 2D-axi and 3D calculations give equivalent results, symmetric and non-symmetric formulations give identical results. Same conclusion can be drawn for other coupled modes. Figure 6 sketches the first eigenmodes shape, in terms of displacement, pressure and free surface elevation: frequency of the decoupled fluid and structure systems are 1.3000 Hz and 1.0355 Hz respectively, while frequency of the first coupled eigenmode is 0.7133 Hz, resulting from a low frequency coupling process (Cho-Song, 2001).

3.2. ELASTO-ACOUSTIC CASE

Validation of the developments in the ANSYS code for elastic-acoustic calculation is performed on the elementary test case sketched by Fig. 7. The geometrical and physical parameters of the problem are as follows: $R = 0.1$m, $R = \alpha R = 0.2$m, $L = H = 0.75$m, $e = 0.01$m, $\rho_s = 7800$ kg/m^3, $E = 2.1\ 10^{11}$ Pa, $\upsilon = 0.3$, $\rho_F = 1000$ kg/m^3, $c = 450$ m/s. Fluid mesh is produced using the same parameters as in the hydroelastic-sloshing case.

a) Fluid problem

For the problem sketched by Fig. 7, eigenfrequencies of the fluid acoustic modes (i.e. fluid modes calculated without taking structure flexibility into account) can be analytically computed according to:

$$f_{l,m,n} = \frac{c}{2\pi} \times \sqrt{\left(\frac{l\pi}{H}\right)^2 + \left(\frac{q_{n,m}}{R}\right)^2} \tag{76}$$

where $q_{n,m}$ is the Mth root of D_n (see appendix A) Index n and l stand for frequency dependency with respect to the θ and z directions, index m stands for the mode rank.

2D axi-3D eigenfrequencies computations are compared with the analytical solution in Tab. 4, for the symmetric component s = 1 of pressure field. Figure 8 sketches the corresponding eigenmodes shapes in terms of pressure distribution for the 2D and 3D model. 2D-axi symmetric calculations are in good agreement with the analytical model and the 3D numerical model. Same observations are drawn for other acoustic modes (for s > 1 and a > 1).

b) Coupled fluid-structure problem

Coupled elasto-acoustic calculations with 2D-axi and 3D finite elements models using symmetric and non-symmetric formulations are compared in Tab. 5: no noticeable discrepancies are observed between all computed frequencies (for symmetric modes of order one). Figure 9 gives the mode shapes for the first decoupled and coupled eigenmodes, illustrating a high frequency coupling process: decoupled structure and fluid (acoustic) frequencies are 327,44Hz and 486,53Hz respectively, the elasto-acoustic frequency for the first mode is 258,14Hz. In the coupled case, Fig. 9 also sketches the fluid pressure and displacement potential iso-values in the 3D model: it is ten checked that spatial repartition of p and φ are identical, as suggested by Eq. (56) which reads $p = \rho_F \omega^2 \varphi$ in the frequency domain.

4. INDUSTRIAL APPLICATION

Calculations presented in the preceding subsection validate the numerical developments carried out in the ANSYS code for modal analysis of coupled problems with pressure-based fluid elements. In particular, enhancement of the existing fluid elements for calculation of fluid acoustic and sloshing modes for 2D axi-symmetric problems has been successfully compared with 3D calculations. Implementation of symmetric coupled formulations has also been validated. In the latter case, practical interest of such coupled formulations is highlighted with the following industrial case, as far as computational time is concerned.

4.1. PROPELLER IN A FLUID

The symmetric coupled formulations implemented in ANSYS are then applied to study an industrial case, in order to perform the modal analysis of a propeller coupled with a fluid.

The eigenmodes and eigenfrequencies will be calculated with the $(\mathbf{u},p)$ and $(\mathbf{u},p,\varphi)$ coupled formulations for two cases, performing the analysis of the propeller coupled with a light (air) and heavy (water) fluid. The water to air frequency ratio $\beta \; \frac{f_{water}}{f_{air}}$ deduced from computations will be compared with experimental data (Sigrist-Le Bras, 2007). Figure 10 sketches the propeller model, the corresponding structure and fluid finite elements. The propeller diameter is Ø = 1.7 m, the fluid domain diameter is about twice the propeller size. The structure domain is meshed with finite elements solid183 (four nodes displacement-formulated elements with quadratic shape functions), while the fluid domain is meshed with finite elements fluid30 (four nodes pressure-formulated elements with linear shape functions). The propeller is made in a aluminum-copper alloy ($CuAl_9Ni_5Fe_4$) physical properties of such a material are ρ_s 7700 kg/m^3, E = ×10^{11} Pa and $\upsilon = 0.3$. Physical properties of the fluid are $\rho_F = 1$kg/m^3, $c = 330$m/s for air and $\rho_F = 1000$ kg/m^3, $c = 1500$ m/s for water.

In the experiments and calculations, the propeller is simply supported on one side of its flange. Besides, only a bounded fluid domain is taken into account in the analysis. As will be seen in the modal analysis presented in the next subsection, the first coupled eigenmodes are low frequency modes, which are characterized by added mass effects. As a consequence, fluid compressibility and acoustic waves are of negligible influence on the coupling process. Therefore, a representation of the far pressure field by a bounded fluid domain with the boundary condition $p = 0$ is valid for the low frequency range. The fluid free surface is also represented with the boundary condition $p = 0$ since gravity waves are also discarded in the analysis.

4.2. MODAL ANALYSIS WITH SYMMETRIC AND NON-SYMMETRIC COUPLED FORMULATIONS

Modal analysis of the propeller is then carried out using the non-symmetric and the symmetric coupled formulations now available with the fluid elements of the ANSYS code. Table 6 gives the numerical results and compares the computed eigenfrequencies for the propeller in air and water. In both cases symmetric and non-symmetric formulations are compared. Figure 11 depicts the mode shapes for eigenmodes #1, #6 and #9, in terms of structure displacement and fluid pressure field on the propeller. The modal analysis shows how added mass effects affect the vibratory behavior of the propeller, as far as the first modes are concerned: frequencies are decreased but no coupling is observed between the propeller blades.

From the numerical point of view, there are no discrepancies between the various coupled formulations, for both cases (air and water). Numerical results are also in good agreement with the experiments, since the computed water/air frequency ratio is close to the experimental one.

From the practical point of view, efficiency of the symmetric formulations is clearly demonstrated when referring to time calculations. Although the size of the problem is almost the same with the two formulations, computational time is reduced from 28.000s to 595s for the coupled case in air by using the symmetric formulation and from 800,000s to 2,000s for the coupled case in water (see Tab. 7): reduction of computational time is rather significant in the present case, but similar results have been observed on other industrial applications (Sigrist, 2006).

Although such a result was expected, since symmetric coupled formulations have precisely been proposed in order to reduce computational costs by using algorithms for symmetric eigenvalue problem, this application example clearly illustrates how coupled fluid-structure modal analysis can benefit from the implementation of symmetric formulations in a finite element code such as ANSYS for industrial purposes.

CONCLUSION

The modal analysis of coupled fluid-structure systems is not a new topic as such, since symmetric coupled formulations were developed more than twenty years ago. However, there is a continuing growing interest to perform modal analysis of complex structures with fluid-structure interaction with industrial finite element codes. In particular, coupled formulations with symmetric matrices are not up to now available in some codes, such as the ANSYS code, which is widely used in industry and academia. In the present paper, numerical developments have been exposed with the view to implementing symmetric formulations in the ANSYS code for the modal analysis of industrial problems with FSI modeling. The basic theory of some symmetric and non-symmetric formulation has first been recalled and validation of their integration in the ANSYS code has been exposed for two generic cases as well as for an industrial problem.

The advantages of using a symmetric formulation have clearly been highlighted, in particular as far as computational time is concerned.

Enhancement of the ANSYS code for the dynamic analysis of fluid-structure interaction problem is still on progress: next step is devoted to the dynamic analysis of coupled systems with modal decomposition techniques (temporal or spectral approaches) using the symmetry properties of the mass and stiffness operators. Validation test cases and industrial applications will be presented in a next paper.

The resented developments in the ANSYS code have been supported by French Naval Shipbuilder DCN for its own applications, but future release of the code will include these new modeling possibilities that will benefit to the entire ANSYS users community in industry for various engineering applications.

REFERENCES

Axisa, F., *Modelling of Mechanical Systems*, Vol. 3: Fluid-Structure Interaction, Elsevier, 2006.

Axisa, F., *Modelling of Mechanical Systems*, Vol. 4.:Flow Induced Vibrations, Elsevier, 2006.

Axisa, F., Gibert, R.J., Non-linear analysis of fluid-structure coupled transient in piping systems, *Pressure Vessel and Piping*, vol. 63, pp. 151-165, 1982.

Bathe, K.J., *Finite Element Procedures in Engineering Analysis*, Prentice-Hall, Englewood Cliffs, 1982.

Bermudez, A., Duran, R., Muschietti, M.A., Rodriguez, R., Solomin, J., Finite element vibration analysis of fluid-solid systems without spurious modes, *Journal of Numerical Analysis*, vol. 32, pp. 1280-1295, 1995.

Bermudez, A., Duran, R., Rodriguez, R., Finite element analysis of compressible and incompressible fluid-solid system, *Mathematics of Computation*, vol. 67, no. 21, pp. 111-136, , 1998.

Biswal, K.C., Bhattacharyya, S.K., Sinha, P.K., Coupled dynamic response of liquid filled composite cylindrical tanks with baffles, *International Mechanical Engineering Congress and Exposition* , New Orleans, 17-22 November 2002.

Cho, J.R., Song, J.M., Assessment of classical numerical models for the separate fluid-structure modal analysis, *Journal of Sound and Vibration*, vol. 239, no. 5, pp. 995-1012, 2001.

Kanarachos, A., Antoniadis, I., Symmetric variational principles and modal methods in fluid-structure interaction problems, *Journal of Sound and Vibration*, vol. 121, no. 1, pp. 77-104, 1998.

Khonke, P., *ANSYS Theory Reference*, Swanson Analysis System, 1986.

Makerle, J., Fluid-structure interaction problems, finite element approach and boundary elements approaches. A bibliography, *Finite Elements in Analysis and Design*, vol. 31, pp. 231-240, 1999.

Morand, H., Ohayon, R., Substructure variational analysis of the vibrations of coupled fluid-structure systems. Finite element results, *International Journal for Numerical Methods in Engineering*, vol. 14, pp. 741-755, 1979.

Morand, H. J-P., Ohayon, R., *Fluid Structure Interaction*, Wiley & Sons, 1995.

Ohayon R., Valid R., True symmetric formulation for fluid-structure interaction in bounded domains. Finite elements results, *Numerical Methods in Coupled Systems*, pp. 293-325, Lewis R.W., Bettes P. & Hinton E. Editors, 1983.

Ohayon, R., Reduced symmetric models for modal analysis of internal structural-acoustic and hydroelastic-sloshing systems, *Computer Methods in Applied Mechanics and Engineering*, vol. 190, pp. 3009-3019, 2001.

Païdoussis, M. P., *Fluid-Structure Interaction: Slender Structures and Axial Flows, vol. 1*, Elsevier, 1998.

Païdoussis, M. P., *Fluid-Structure Interaction: Slender Structures and Axial Flows, vol. 2*, Elsevier, 2003.

Rajakumar, C., Rogers, C.G., The Lanczos algorithm applied to unsymmetric generalized eigenvalue problem, *International Journal of Numerical Methods in Engineering*, vol. 32, pp. 1009-1026, 1991.

Schäfer, M., Teschauer, I., Numerical simulation of coupled fluid-solid problems, *Computer Methods in Applied Mechanics and Engineering*, vol. 190, pp. 3645-3667, 2001.

Sigrist, J.F., Lainé, C., Peseux, B., Dynamic analysis of a coupled fluid-structure problem with fluid sloshing, *Pressure Vessel and Piping, vol*. 489, pp. 149-156, 2004.

Sigrist, J.F., Broc, D., Dynamic analysis of a nuclear reactor with fluid-structure interaction: part I seismic loading, fluid added mass and added stiffness, (in press) *Nuclear Engineering and Design*, 2006.

Sigrist, J.F., 2006. Symmetric and non-symmetric formulations for fluid-structure interaction problems: reference test cases for numerical developments in commercial finite element code, *Pressure Vessel and Piping*, Vancouver, July 25-28, 2006.

Sigrist, J.F., Le Bras, Y., Experimental and numerical modal analysis of a propeller, (submitted to) *Navy and Shipbuilding Nowadays*, St. Petersburg, June 26-29, 2007.

Hamdi, M.A., Ousset, Y., Verchery, G., A displacement method for the analysis of vibrations of coupled fluid-structure systems, *International Journal of Numerical Methods in Engineering*, vol. 13, pp. 139-150, 1978.

Woyak, D.B., *Acoustic and Fluid Structure Interaction*, Swanson Analysis System, 1995.

APPENDIX

Analytical calculation of sloshing and acoustic modes of require the computation of first roots of function $D_{\alpha,n}(x) = J'_n(x)\, Y'_n(\alpha x) - Y'_n(x)\, J'_n(\alpha x)$ where J'_n and Y'_n are the derivates of the first and second kind Bessel functions of order n. Figure 12 gives a graphical representation of function $D_{\alpha,n}$ for $\alpha = 2$ n = 1 . Table 8 gives the first roots of $D_{\alpha,n}$ in the range [0,10].

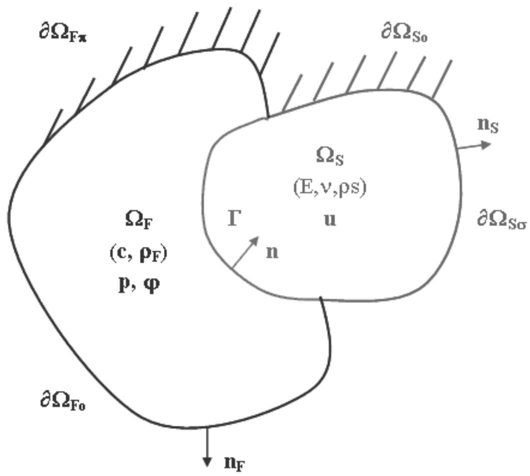

Figure 1 General representation of a fluid-structure interaction problem

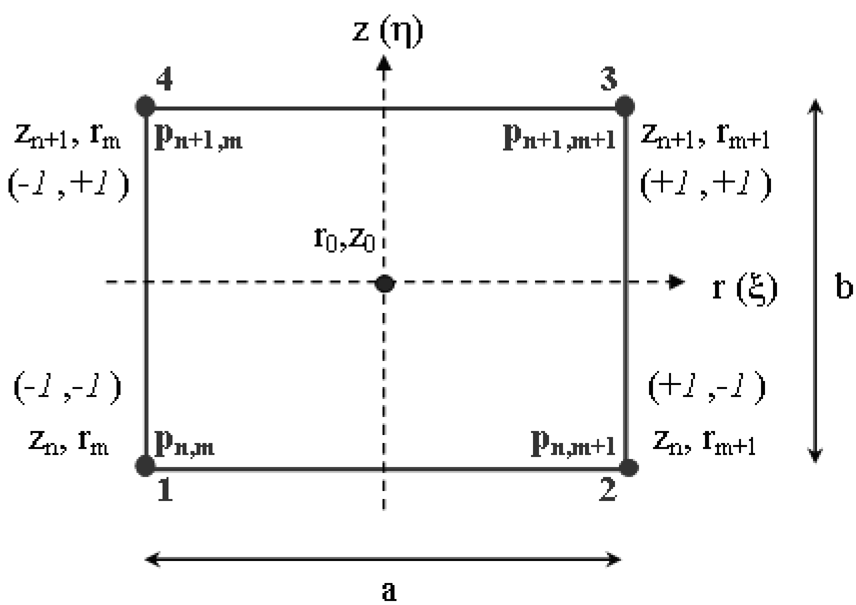

Figure 2 Axi-symmetric pressure-based fluid finite element

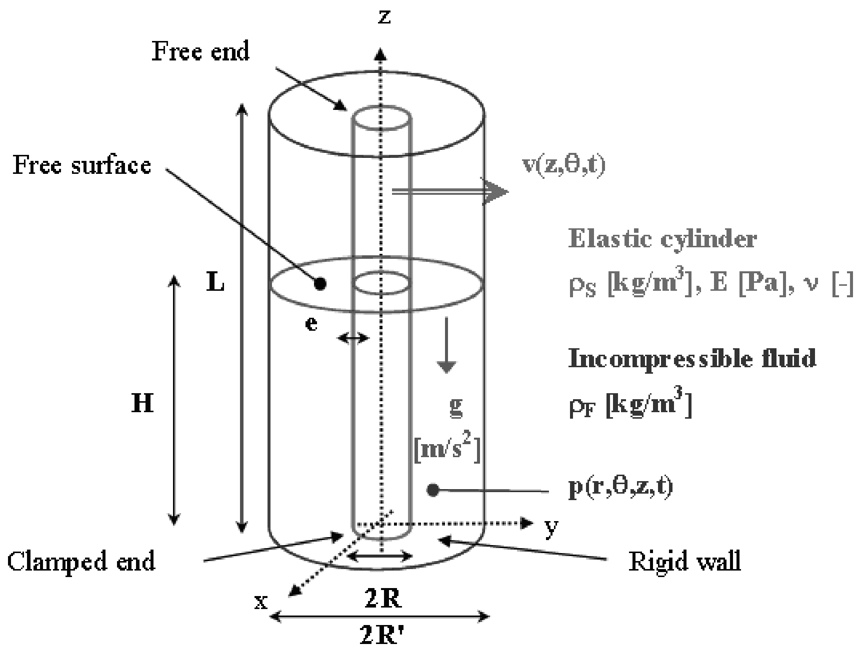

Figure 3 Elementary validation test case. Hydro-elastic coupling with fluid free surface

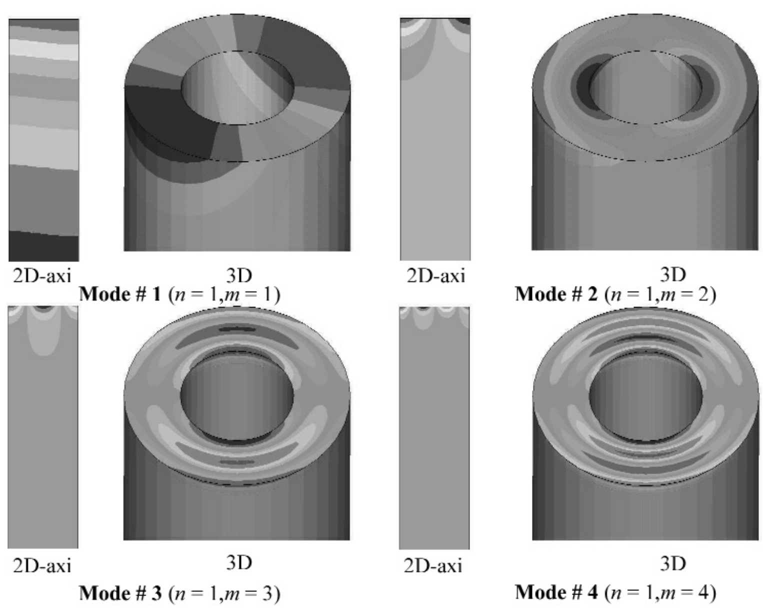

Figure 4 Fluid sloshing modes. 3D and 2D-axi symmetric finite element calculation

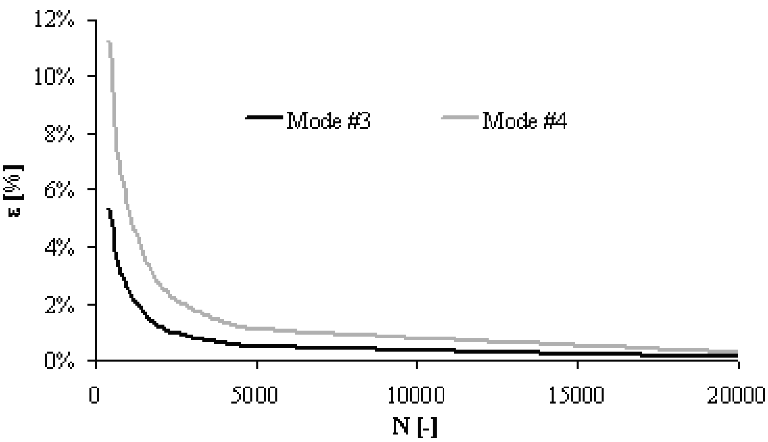

Figure 5 Fluid sloshing modes. Convergence of frequencies for sloshing modes #3 and #4 with mesh refinement

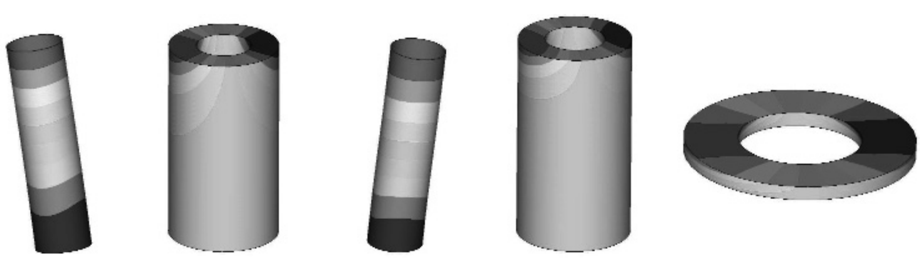

Figure 6 Validation test case. Uncoupled and coupled hydro-elastic mode

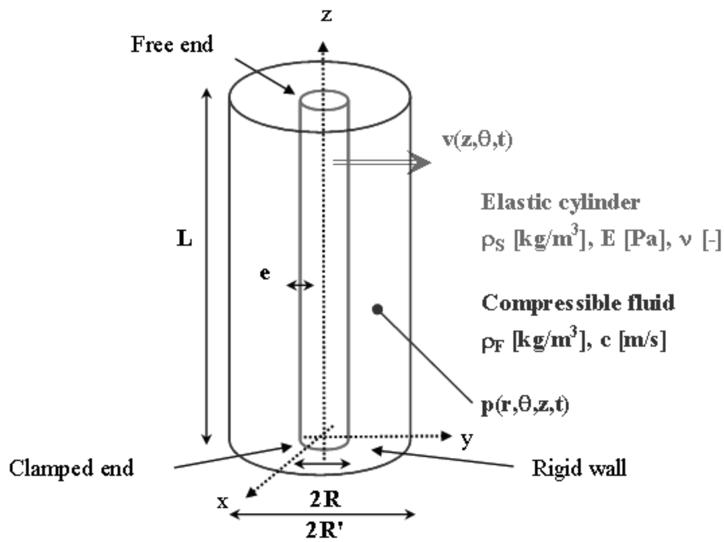

Figure 7 Elementary validation test case. Elasto-acoustic coupling without fluid free surface

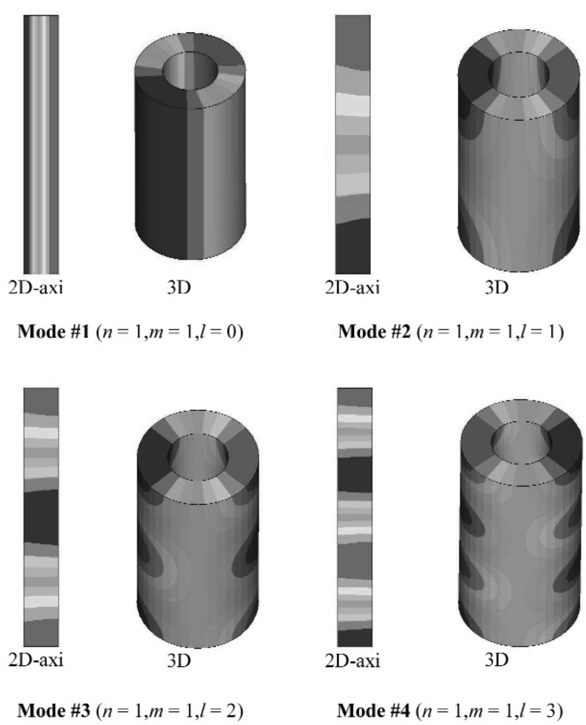

Figure 8 Fluid acoustic modes. 3D and 2D-axi symmetric finite element calculation

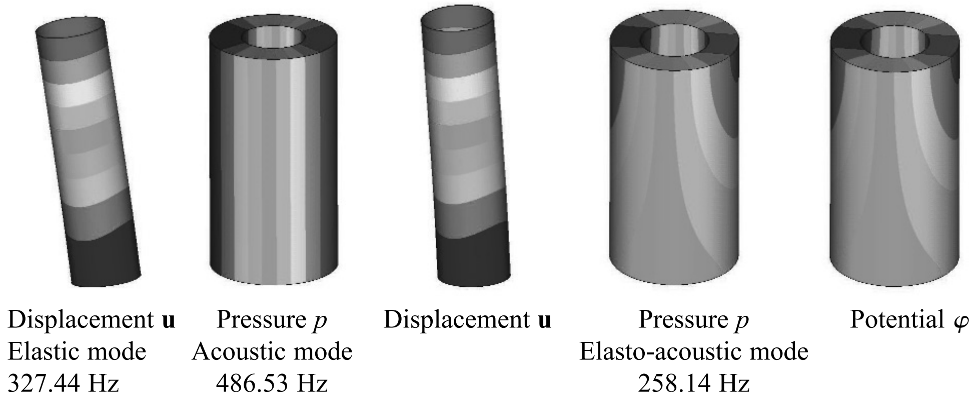

Figure 9 Validation test case. Uncoupled and coupled elasto-acoustic mode

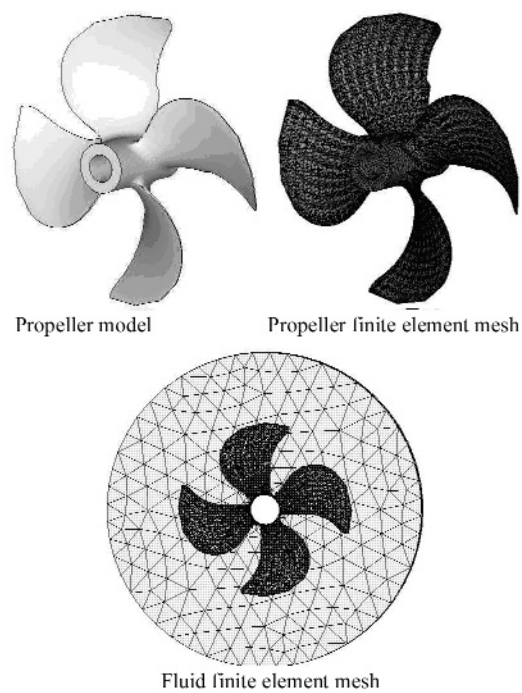

Figure 10 Propeller and fluid finite element model

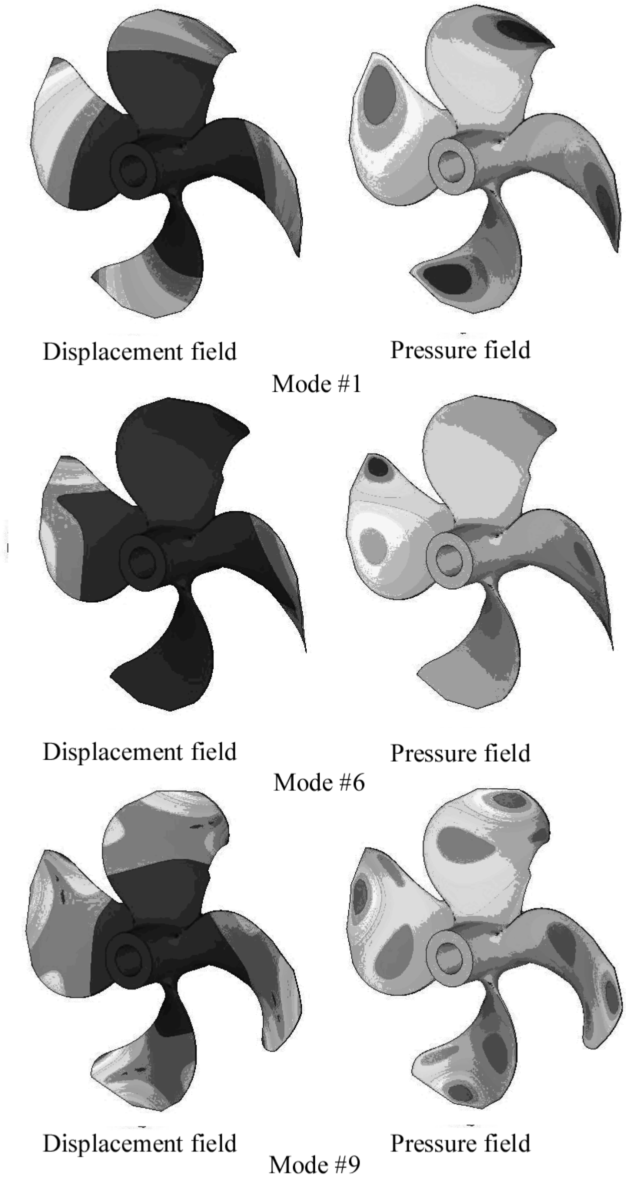

Figure 11 Propeller eigenmodes in water (coupled calculation with (u,p,φ) symmetric formulation)

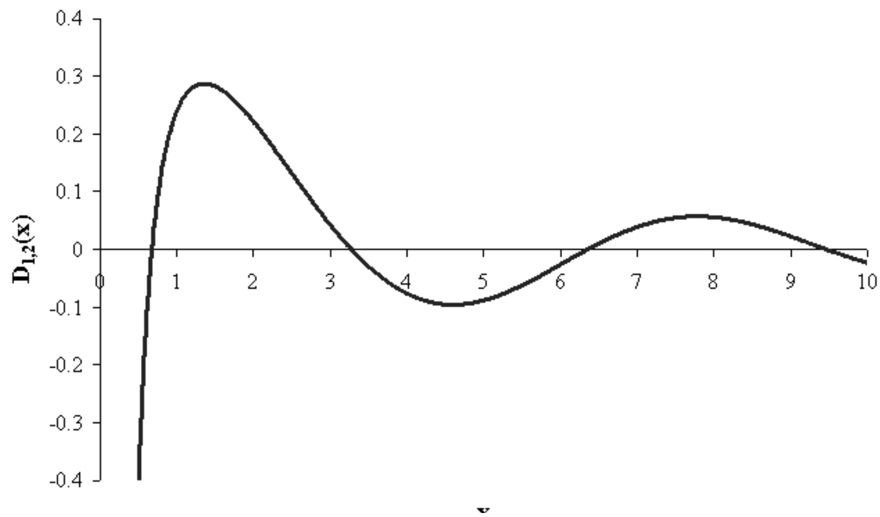

Figure 12 Graphical representation of function x–$D_{\alpha,n(x)}$ for $n = 1$, $\alpha = 2$, and $x \in [0,10]$

Table 1. Coupled fluid-structure analysis with the ANSYS code, using fluid displacement-based or pressure-based formulations

	(u,ξ) coupled formulation	**(u,*p*) coupled formulation**
Fluid acoustic modes	×	×
Fluid sloshing modes	×	O
2D axi-symmetric geometry	×	O
3D geometry	×	×
Modal analysis	×	×
Static analysis	×	×
Dynamic analysis, direct method	×	×
Dynamic analysis, modal method	×	O

Table 2. Validation test case. Fluid sloshing modes with pressure-based formulation. 3D and 2D axi-symmetric results

Frequency	**Analytical solution**	**3D finite element model**		**2D axi-symmetric finite element model**	
f1	1.2973 Hz	1.3000 Hz	*+0.21%*	1.2981 Hz	*+0.06%*
f2	2.8559 Hz	2.9027 Hz	*+1.64%*	2.8978 Hz	*+1.47%*
f3	3.9731 Hz	4.1930 Hz	*+5.53%*	4.1850 Hz	*+5.33%*
f4	4.8511 Hz	5.4810 Hz	*+12.98%*	5.3970 Hz	*+11.25%*

Table 3. Validation test case. Coupled hydro-elastic modes with symmetric and non-symmetric formulation. 3D and 2D axi-symmetric results

Frequency	2D-axi		3D	
	($\mathbf{u}$,p)	($\mathbf{u}$,η,φ)	($\mathbf{u}$,p)	($\mathbf{u}$,η,φ)
f_1	0.7133 Hz	0.7133 Hz	0.7127 Hz	0.7127 Hz
f_2	1.4829 Hz	1.4829 Hz	1.4837 Hz	1.4837 Hz
f_3	2.8860 Hz	2.8860 Hz	2.8907 Hz	2.8907 Hz
f_4	3.5832 Hz	3.5832 Hz	3.5809 Hz	3.5809 Hz

Table 4. Validation test case. Fluid acoustic modes with pressure-based formulation. 3D and 2D axi-symmetric results

Frequency	Analytical solution	3D finite element model		2D axi-symmetric finite element model	
f_1	1617.0	1621.8	*+0.30%*	1617.0	*0.00%*
f_2	1901.3	1905.5	*+0.23%*	1901.5	*+0.02%*
f_3	2571.9	2577.8	*+0.23%*	2574.8	*+0.11%*
f_4	3408.0	3421.2	*+0.39%*	3418.9	*+0.32%*

Table 5. Validation test case. Coupled elasto-acoustic modes with symmetric and non-symmetric formulation. 3D and 2D axi-symmetric results

Frequency	2D-axi		3D	
	($\mathbf{u}$,p)	($\mathbf{u}$,p,φ)	($\mathbf{u}$,p)	($\mathbf{u}$,p,φ)
f_1	258.14 Hz	258.14 Hz	257.82 Hz	257.82 Hz
f_2	558.38 Hz	558.38 Hz	559.48 Hz	559.48 Hz
f_3	639.47 Hz	639.47 Hz	640.34 Hz	640.34 Hz
f_4	791.60 Hz	791.60 Hz	792.48 Hz	792.48 Hz

Table 6. Propeller eigenfrequencies in air and water. Coupled calculation with ($\mathbf{u}$,p) and ($\mathbf{u}$,p,φ) formulations. Numerical and experimental air/water eigenfrequency ratio comparisons

Frequency	Fluid: air		Fluid: water		β num.	β exp.
	($\mathbf{u}$,p)	($\mathbf{u}$,p,φ)	($\mathbf{u}$,p)	($\mathbf{u}$,p,φ)		
f_1	64.82 Hz	64.92 Hz	34.67 Hz	34.90 Hz	46.5 %	45.2%
f_6	109.98 Hz	110.11 Hz	64.79 Hz	65.07 Hz	41.1 %	39.1%
f_9	179.98 Hz	179.24 Hz	119.27 Hz	119.60 Hz	33.7 %	33.2%

Table 7. Problem size and computational time with $(\mathbf{u},p)$ and $(\mathbf{u},p,\varphi)$ formulations for coupled eigenfrequencies calculation

	$(\mathbf{u},p)$ formulation		**$(\mathbf{u},p,\varphi)$ formulation**	
	Fluid: air	Fluid: water	Fluid: air	Fluid: water
Number of DOF	236.602		251.171	
CPU Time	28.469 s	788.434 s	595 s	2174 s

Table 8. First roots of function $D_{\alpha,n}$ for $n = 1$ and $\alpha = 2$

$\boldsymbol{m}$	**1**	**2**	**3**	**4**
$q_{m,n=1}$	0.677360	3.2824712	6.3532112	9.4713290

Announcement and Call for Papers

MULTIPHYSICS 2007

12-14 December 2007
Manchester, UK

Multiphyiscs analysis has become increasingly important in recent years due to demand in design and understanding of complex systems.

The objective of the conference is to share and explore findings on mathematical advances, numerical modelling and experimental validation of theoretical and practical systems in a wide range of applications.

Authors are invited to submit abstracts of papers up to 300 words containing key objectives and conclusions.

Abstracts should contain the title of the presentation, names of authors, their affiliations including the full contact details of the corresponding author, and some keywords.

Abstract submissions should be made to
email conference@multiphysics.org
or online www.multiphysics.org
by 31st May 2007

Authors of selected abstracts will be invited to submit full length papers for publication in
'*The International Journal of Multiphysics*'.